

Wave response of an ice floe of arbitrary geometry

Michael H. Meylan

Institute of Information and Mathematical Sciences, Massey University, Auckland, New Zealand

Received 7 November 2000; revised 29 May 2001; accepted 13 September 2001; published 5 January 2002.

[1] A fully three-dimensional model for the motion and bending of a solitary ice floe due to wave forcing is presented. This allows the scattering and wave-induced force for a realistic ice floe to be calculated. These are required to model wave scattering and wave-induced ice drift in the marginal ice zone. The ice floe is modeled as a thin plate, and its motion is expanded in the thin plate modes of vibration. The modes are substituted into the integral equation for the water. This gives a linear system of equations for the coefficients used to expand the ice floe motion. Solutions are presented for the ice floe displacement, the scattered energy, and the time-averaged force for a range of ice floe geometries and wave periods. It is found that ice floe stiffness is the most important factor in determining ice floe motion, scattering, and force. However, above a critical value of stiffness the floe geometry also influences the scattering and force. *INDEX TERMS:* 4540 Oceanography: Physical: Ice mechanics and air/sea/ice exchange processes, 4560 Oceanography: Physical: Surface waves and tides (1255), 9310 Information Related to Geographic Region: Antarctica, 9315 Information Related to Geographic Region: Arctic region

1. Introduction

[2] It is widely recognized that understanding the relationship between ocean waves and sea ice requires a fully three-dimensional model for the motion and bending of a solitary ice floe [Squire *et al.*, 1995]. Such an ice floe model is derived in this paper. The model includes flexure and is for an ice floe of arbitrary shape. It allows the wave scattering and wave-induced force for a realistic ice floe to be calculated for the first time.

[3] The marginal ice zone (MIZ) is an interfacial region, composed of an aggregate of ice and water, which forms at the boundary of open and ice-covered seas. The major interaction between open and ice-covered seas is through waves. These waves are generated in the open water and are responsible for breaking up the continuous pack ice. For waves to reach the continuous pack ice, they must pass through the MIZ.

[4] Experimental measurements have shown that as ocean waves pass through the MIZ, their character is radically altered. Wadhams *et al.* [1988] and Squire and Moore [1980] found that there was strong and significant exponential attenuation of wave energy. This attenuation decreased with increasing wave period. The angular spreading of incoming ocean waves was measured by Wadhams *et al.* [1986], who found that from a narrow directional spectrum in the open water the directional wave spectrum evolves to become isotropic within the MIZ. Experimental measurements of the motion of individual ice floes have shown that ice floe bending is significant. Squire [1983] and Squire and Martin [1980] measured the motion of ice floes using strain gauges. They showed that ice floe flexure is significant and must be included in ice floe models.

[5] Masson and LeBlond [1989] and Meylan *et al.* [1997] have derived models for the propagation of waves through the MIZ on the basis of the linear transport equation. These models predict the exponential decay and directional spreading of the incoming wave spectrum qualitatively. However, they were quantitatively inaccurate because neither of them used a realistic model to calculate the individual ice floe scattering. This was because no realistic model existed. Masson and LeBlond [1989] and Masson [1991] assumed

that the ice floe was a rigid body. Wadhams [1986] included ice floe flexure, but the model was two-dimensional, and the solution was only calculated approximately. While Meylan and Squire [1994] solved the Wadhams problem exactly, two-dimensional models give no information about the directional scattering and so cannot be used in wave scattering models. Meylan and Squire [1996] extended the two-dimensional model to three dimensions but only for the unrealistic case of a circular ice floe. This was the ice floe model used by Meylan *et al.* [1997].

[6] In this paper a fully three-dimensional model for the motion and bending of a solitary ice floe is developed as follows. The ice floe motion is expanded in the free modes of vibration (the modes of vibration of the ice floe in the absence of the water). These modes must be determined numerically, and this is done by using the finite element method. The equations of motion for the water are transformed into an integral equation over the wetted surface of the ice floe. This transformation was developed by John [1949, 1950] and is standard in offshore engineering [Sarpkaya and Isaacson, 1981]. The free modes of vibration are then substituted into the integral equation for the water. This gives a linear system of equations for the coefficients used to expand the floe motion.

[7] Solutions are presented for the ice floe displacements, the scattering of wave energy, and the wave-induced force for a range of ice floe geometries and wave periods. The scattering is considered because of its importance in MIZ scattering models [Masson and LeBlond, 1989; Meylan *et al.*, 1997]. The wave-induced force is included because of the importance of this term in models of ice floe drift.

2. Equation of Motion for the Ice Floe

[8] Ice floes range in size from much smaller to much larger than the dominant wavelength of the ocean waves. However, there are two reasons why solutions for ice floes of intermediate size (a size similar to the wavelength) are the most important. The first is that at these intermediate sizes ice floes scatter significant wave energy. The second is that since it is wave-induced flexure that determines the size of ice floes in the MIZ, ice floes tend to form most often at this intermediate length.

[9] The theory for an ice floe of intermediate size which is developed in this paper obviously also applies to small or large

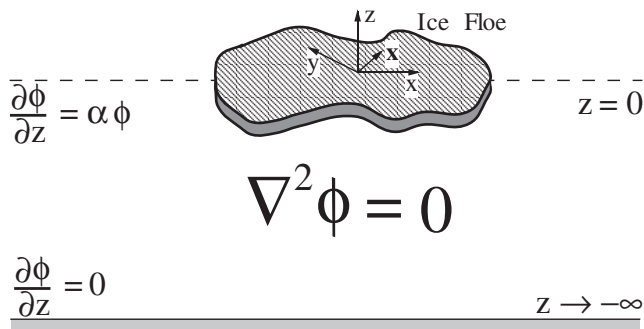


Figure 1. The schematic diagram of the boundary value problem and the coordinate system used in the solution.

floes. However, if the solution for a small or large floe is required, then the appropriate simpler theory should be used. Small ice floes (ice floes much smaller than the wavelength) should be modeled as rigid [Masson and LeBlond, 1989; Masson, 1991]. Large ice floes (ice floes much larger than the wavelength) should be modeled as infinite and flexible [Fox and Squire, 1994]. In the intermediate region, where the size of the wavelength is similar to the size of the ice floe, the ice floe must be modeled as finite and flexible.

[10] We model the ice floe as a thin plate of constant thickness and shallow draft following Wadhams [1986] and Squire et al.

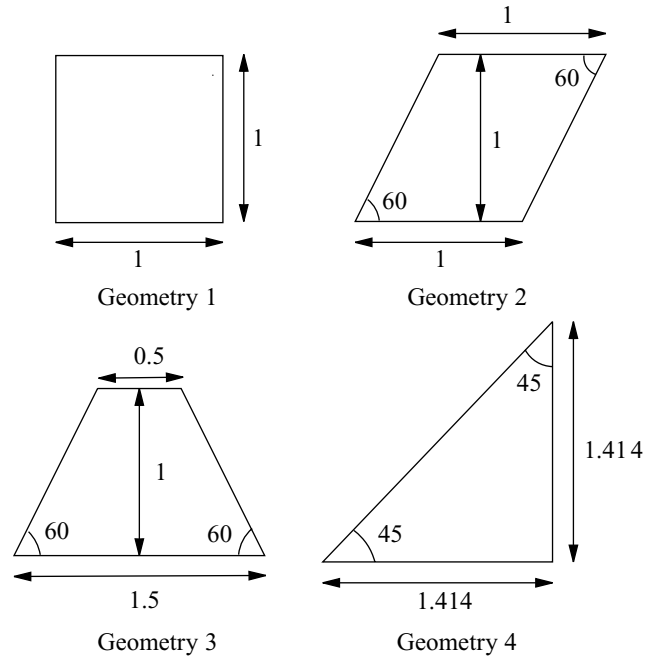


Figure 2. The four ice floe geometries for which solutions will be calculated and their numbering.

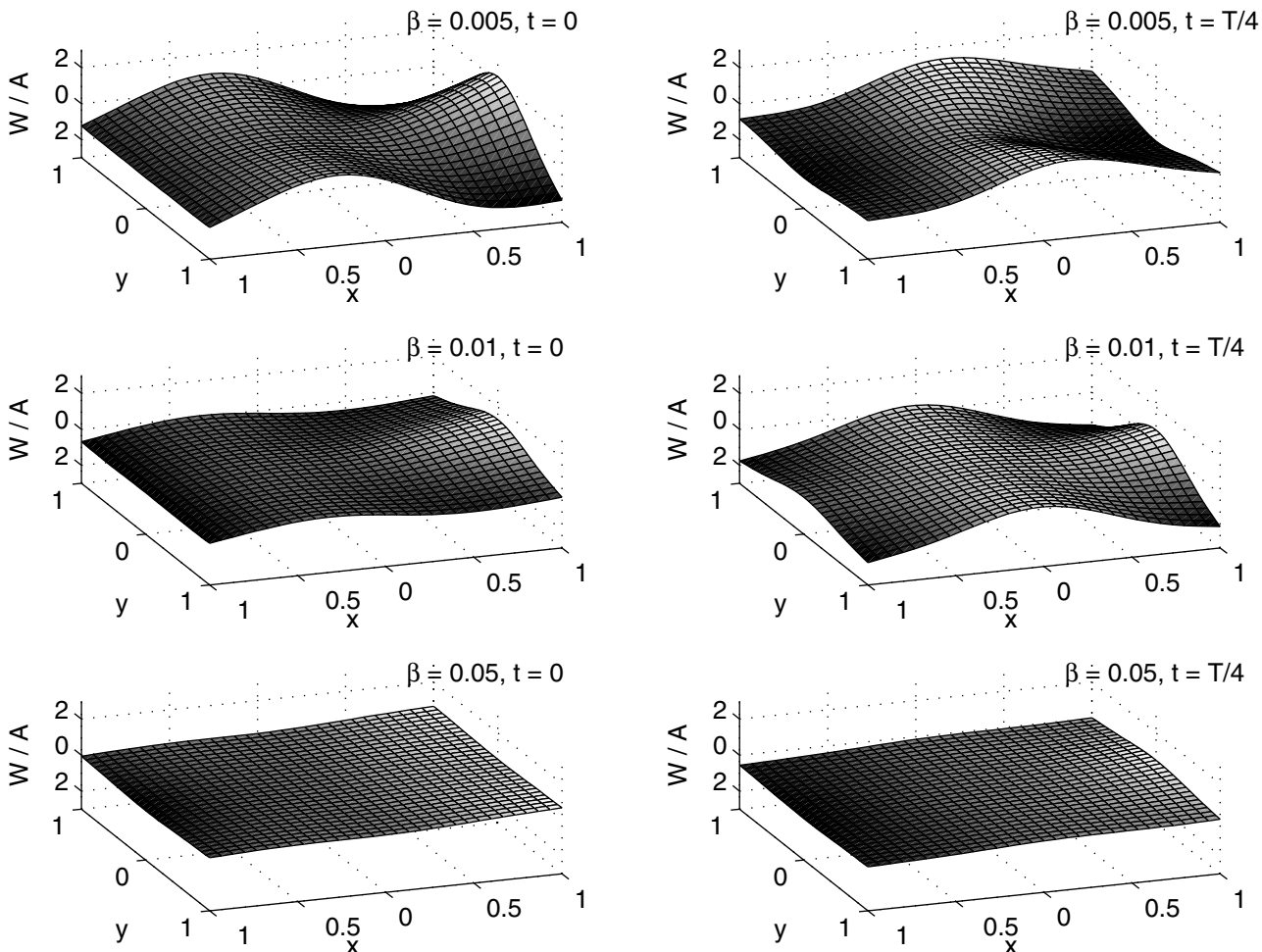


Figure 3. The displacement of an ice floe of geometry 1 for the times and stiffness shown. The mass was $\gamma = 0.005$, the wave number was $\alpha = \pi$, and the wave was traveling in the positive x direction.

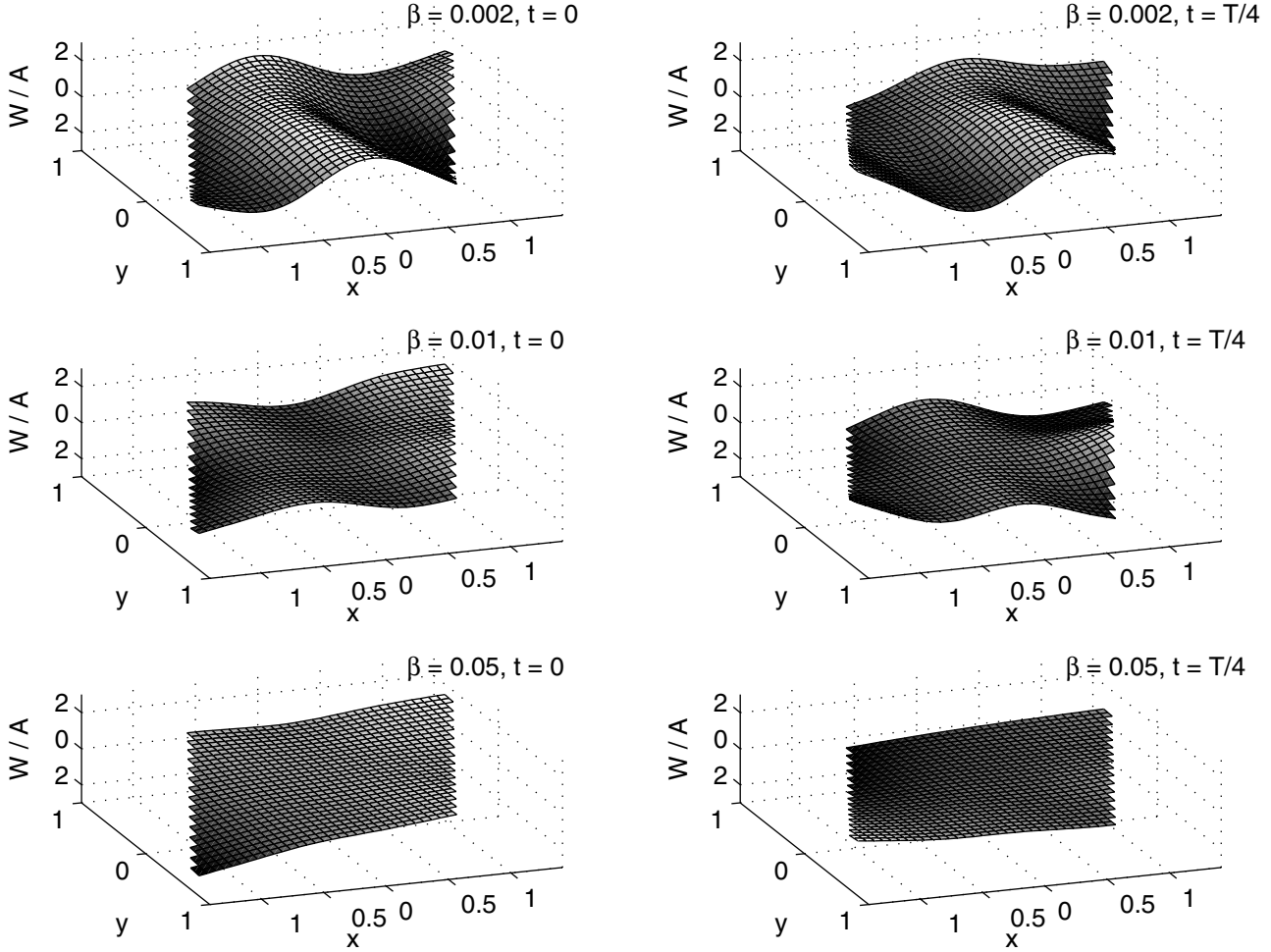


Figure 4. The displacement of an ice floe of geometry 2 for the times and stiffness shown. The mass was $\gamma = 0.005$, the wave number was $\alpha = \pi$, and the wave was traveling in the positive x direction.

[1995]. The thin plate equation [Hildebrand, 1965] gives the following equation of motion for the ice floe:

$$D\nabla^4 W + \rho_i h \frac{\partial^2 W}{\partial t^2} = p, \quad (1)$$

where W is the floe displacement, ρ_i is the floe density, h is the floe thickness, p is the pressure, and D is the modulus of rigidity of the floe ($D = Eh^3/12(1 - \nu^2)$, where E is the Young's modulus and ν is Poisson's ratio). Visco-elastic effects can be included by making D have some imaginary (damping) component, but this will not be done here to keep the presented results simpler. We assume that the plate is in contact with the water at all times so that the water surface displacement is also W . Equation (1) is subject to the free edge boundary conditions for a thin plate:

$$\frac{\partial^2 W}{\partial n^2} + \nu \frac{\partial^2 W}{\partial s^2} = 0, \quad \text{and} \quad \frac{\partial^3 W}{\partial n^3} + (2 - \nu) \frac{\partial^3 W}{\partial n \partial s^2} = 0 \quad (2)$$

[Hildebrand, 1965], where n and s denote the normal and tangential directions, respectively.

[11] The pressure, p , is given by the linearized Bernoulli's equation at the water surface,

$$p = -\rho \frac{\partial \Phi}{\partial t} - \rho g W, \quad (3)$$

where Φ is the velocity potential of the water, ρ is the density of the water, and g is the acceleration due to gravity.

[12] We now introduce nondimensional variables. We nondimensionalize the length variables with respect to a where the surface area of the floe is $4a^2$. We nondimensionalize the time variables with respect to $\sqrt{g/a}$ and the mass variables with respect to ρa^3 . The nondimensional variables, denoted by an overbar, are

$$\bar{x} = \frac{x}{a}, \quad \bar{y} = \frac{y}{a}, \quad \bar{z} = \frac{z}{a}, \quad \bar{W} = \frac{W}{a}, \quad \bar{t} = t \sqrt{\frac{g}{a}}, \quad \text{and} \quad \bar{\Phi} = \frac{\Phi}{a \sqrt{ag}}.$$

In the nondimensional variables, (1) and (3) become

$$\beta \nabla^4 \bar{W} + \gamma \frac{\partial^2 \bar{W}}{\partial \bar{t}^2} = \frac{\partial \bar{\Phi}}{\partial \bar{t}} - \bar{W}, \quad (4)$$

where

$$\beta = \frac{D}{\rho a^4} \quad \text{and} \quad \gamma = \frac{\rho_i h}{\rho a}.$$

We shall refer to β and γ as the stiffness and mass, respectively.

[13] We will determine the response of the ice floe to wave forcing of a single frequency (the response for more complex wave forcing can be found by superposition of the single-frequency solutions). Since the equations of motion are linear, the displacement and potential must have the same single-fre-

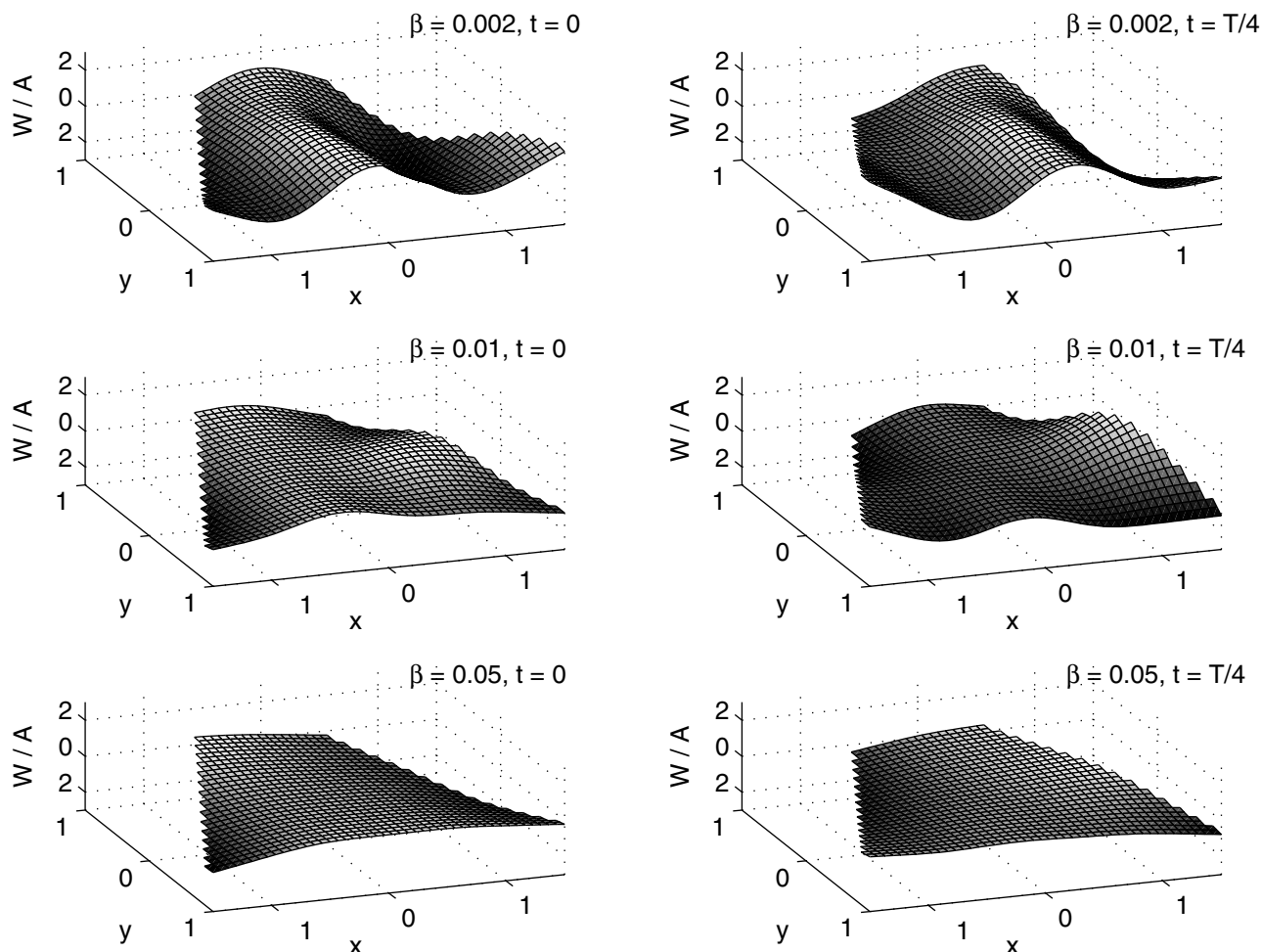


Figure 5. The displacement of an ice floe of geometry 3 for the times and stiffness shown. The mass was $\gamma = 0.005$, the wave number was $\alpha = \pi$, and the wave was traveling in the positive x direction.

quency dependence. Therefore they can be expressed as the real part of a complex quantity whose time dependence is $e^{-i\sqrt{\alpha}t}$, where α is the nondimensional wave number, and we write $\bar{W}(\bar{x}, \bar{y}, \bar{t}) = \text{Re}[w(\bar{x}, \bar{y})e^{-i\sqrt{\alpha}t}]$ and $\bar{\Phi}(\bar{x}, \bar{y}, \bar{z}, \bar{t}) = \text{Re}[\phi(\bar{x}, \bar{y}, \bar{z})e^{-i\sqrt{\alpha}t}]$. In the complex variables the equation of motion of the ice floe (4) is

$$\beta \nabla^4 w + \alpha \gamma w = \sqrt{\alpha} \phi - w. \quad (5)$$

From now on, we will drop the overbar and assume all variables are nondimensional.

3. Equations of Motion for the Water

[14] We require the equation of motion for the water to solve (5). We begin with the nondimensional equations of potential theory which describe linear surface gravity waves

$$\left. \begin{aligned} \nabla^2 \phi &= 0, & -\infty < z < 0, \\ \partial \phi / \partial z &= 0, & z \rightarrow -\infty, \\ \partial \phi / \partial z &= -i\sqrt{\alpha} w, & z = 0, \mathbf{x} \in \Delta, \\ \partial \phi / \partial z - \alpha \phi &= p, & z = 0, \mathbf{x} \notin \Delta \end{aligned} \right\} \quad (6)$$

[Wehausen and Laitone, 1960]. As before, w is the displacement of the floe and p is the pressure at the water surface. The vector

$\mathbf{x} = (x, y)$ is a point on the water surface and Δ is the region of the water surface occupied by the floe. The water is assumed infinitely deep. A schematic diagram of this problem is shown in Figure 1.

[15] The boundary value problem (6) is subject to an incident wave which is imposed through a boundary condition as $|\mathbf{x}| \rightarrow \infty$. This boundary condition, which is called the Sommerfeld radiation condition, is essentially that at large distances the potential consists of a radial outgoing wave (the wave generated by the ice floe motion) and the incident wave. It is expressed mathematically as

$$\lim_{|\mathbf{x}| \rightarrow \infty} \sqrt{|\mathbf{x}|} \left(\frac{\partial}{\partial |\mathbf{x}|} - i\alpha \right) (\phi - \phi^{\text{in}}) = 0 \quad (7)$$

[Wehausen and Laitone, 1960]. The incident potential (i.e., the incoming wave) ϕ^{in} is

$$\phi^{\text{in}}(x, y, z) = \frac{A}{\sqrt{\alpha}} e^{i\alpha(x \cos \theta + y \sin \theta)} e^{\alpha z}, \quad (8)$$

where A is the nondimensional wave amplitude.

[16] The standard solution method to the linear wave problem is to transform the boundary value problem into an integral equation using a Green function [John, 1949, 1950; Sarpkaya

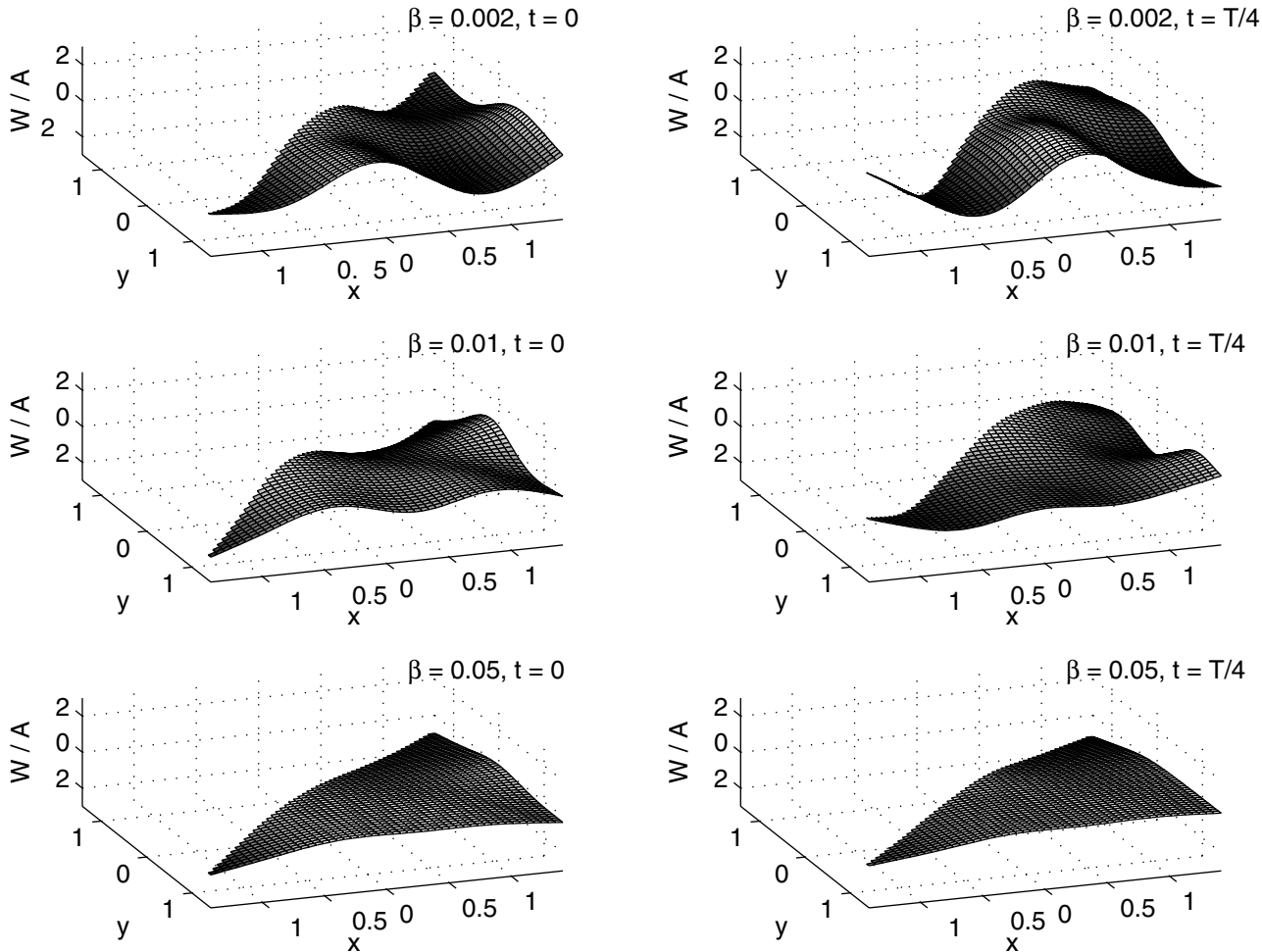


Figure 6. The displacement of an ice floe of geometry 4 for the times and stiffness shown. The mass was $\gamma = 0.005$, the wave number was $\alpha = \pi$, and the wave was traveling in the positive x direction.

and Isaacson, 1981; Meylan and Squire, 1996]. Performing such a transformation, the boundary value problems (6) and (7) become

$$\phi(\mathbf{x}) = \phi^i(\mathbf{x}) + \iint_{\Delta} G_{\alpha}(\mathbf{x}; \mathbf{y}) (\alpha \phi(\mathbf{x}) + i\sqrt{\alpha} w(\mathbf{x})) dS_{\mathbf{y}}. \quad (9)$$

The Green function G_{α} is

$$G_{\alpha}(\mathbf{x}; \mathbf{y}) = \frac{1}{4\pi} \left(\frac{2}{|\mathbf{x} - \mathbf{y}|} - \pi \alpha (\mathbf{H}_0(\alpha|\mathbf{x} - \mathbf{y}|) + Y_0(\alpha|\mathbf{x} - \mathbf{y}|)) + 2\pi i \alpha J_0(\alpha|\mathbf{x} - \mathbf{y}|) \right),$$

[Wehausen and Laitone, 1960; Meylan and Squire, 1996] where J_0 and Y_0 are Bessel functions of the first and second kind, respectively, of order zero, and \mathbf{H}_0 is the Struve function of order zero [Abramowitz and Stegun, 1964]. A solution for water of finite depth could be found by simply using the depth-dependent Green function [Wehausen and Laitone, 1960].

[17] The integral equation (9) will be solved using numerical integration. The only difficulty arises from the nontrivial nature of the kernel of the integral equation (the Green function). However, the Green function has no z dependence because of the shallow draft approximation and depends only on $|\mathbf{x} - \mathbf{y}|$. This means that the Green function is one dimensional and the

values which are required for a given calculation can be looked up in a previously computed table.

4. Solving for the Wave-Induced Ice Floe Motion

[18] To determine the ice floe motion, we must solve (5) and (9) simultaneously. We do this by expanding the floe motion in the free modes of vibration of a thin plate. The major difficulty with this method is that the free modes of vibration can be determined analytically only for very restrictive geometries, for instance, a circular thin plate. Even the free modes of vibration of a square plate with free edges must be determined numerically. This is the reason why the solution of Meylan and Squire [1996] was only for a circular floe.

[19] Since the operator ∇^4 , subject to the free edge boundary conditions, is self adjoint, a thin plate must possess a set of modes w_i which satisfy the free boundary conditions and the following eigenvalue equation:

$$\nabla^4 w_i = \lambda_i w_i.$$

The modes which correspond to different eigenvalues λ_i are orthogonal, and the eigenvalues are positive and real. While the plate will always have repeated eigenvalues, orthogonal modes can

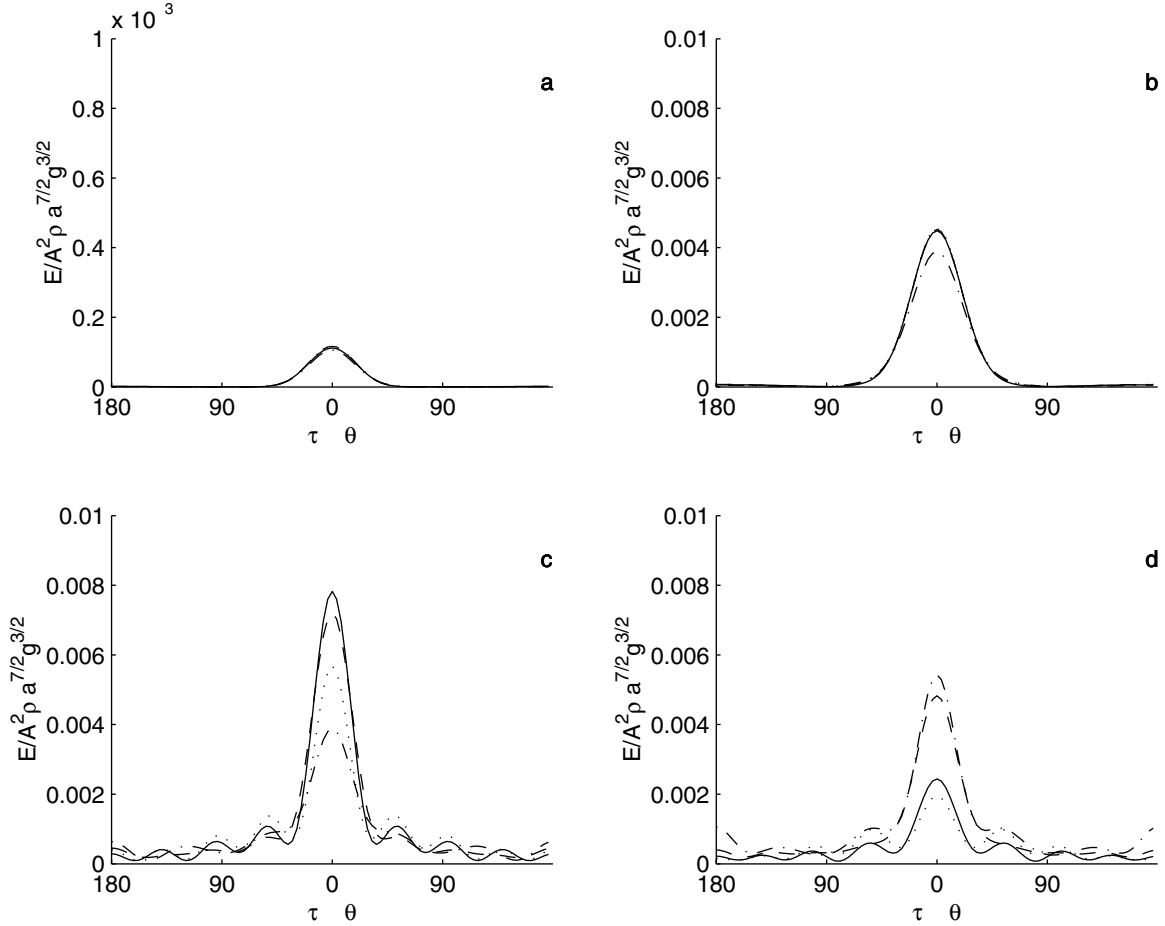


Figure 7. The scattering as a function of angle for ice floe geometries 1 (solid lines), 2 (dashed lines), 3 (dashed-dotted lines), and 4 (dotted lines). The values of the stiffness are (a) $\beta = 0.0004$, (b) $\beta = 0.002$, (c) $\beta = 0.01$, and (d) $\beta = 0.05$, with $\alpha = \pi$ and $\gamma = 0.005$.

still be found and the modes can be normalized. We therefore assume that the modes are orthonormal, i.e.,

$$\iint_{\Delta} w_i(\mathbf{Q}) w_j(\mathbf{Q}) dS_{\mathbf{Q}} = \delta_{ij},$$

where δ_{ij} is the Kronecker delta. The eigenvalues λ_i have the property that $\lambda_i \rightarrow \infty$ as $i \rightarrow \infty$, and we order the modes by increasing eigenvalue. These modes can be used to expand any function over the wetted surface of the ice floe Δ .

[20] We expand the displacement of the floe in a finite number of modes N , i.e.,

$$w(\mathbf{x}) = \sum_{i=1}^N c_i w_i(\mathbf{x}). \quad (10)$$

From the linearity of (9) the potential can be written in the following form:

$$\phi = \phi_0 + \sum_{i=1}^N c_i \phi_i, \quad (11)$$

where ϕ_0 and ϕ_i satisfy the integral equations

$$\phi_0(\mathbf{x}) = \phi^{\text{in}}(\mathbf{x}) + \iint_{\Delta} \alpha G_{\alpha}(\mathbf{x}; \mathbf{y}) \phi(\mathbf{y}) dS_{\mathbf{y}} \quad (12)$$

and

$$\phi_i(\mathbf{x}) = \iint_{\Delta} G_{\alpha}(\mathbf{x}; \mathbf{y}) (\alpha \phi_i(\mathbf{x}) + i\sqrt{\alpha} w_i(\mathbf{y})) dS_{\mathbf{y}}. \quad (13)$$

The potential ϕ_0 represents the potential due the incoming wave assuming that the displacement of the ice floe is zero. The potentials ϕ_i represent the potential which is generated by the plate vibrating with the i th mode in the absence of any input wave forcing.

[21] We substitute (10) and (11) into (5) to obtain

$$\beta \sum_{i=1}^N \lambda_i c_i w_i - \alpha \gamma \sum_{i=1}^N c_i w_i = i\sqrt{\alpha} \left(\phi_0 + \sum_{i=1}^N c_i \phi_i \right) - \sum_{i=1}^N c_i w_i. \quad (14)$$

To solve (14), we multiply by w_j and integrate over the plate (i.e., we take the inner product with respect to w_j) taking into account the orthogonality of the modes w_i , and obtain

$$\beta \lambda_j c_j + (1 - \alpha \gamma) c_j = \iint_{\Delta} i\sqrt{\alpha} \left(\phi_0(\mathbf{Q}) + \sum_{i=1}^N c_i \phi_i(\mathbf{Q}) \right) w_j \times (\mathbf{Q}) dS_{\mathbf{Q}}, \quad (15)$$

which is a matrix equation in c_i .

[22] We cannot solve (15) without determining the modes of vibration of the thin plate w_i (along with the associated eigen-

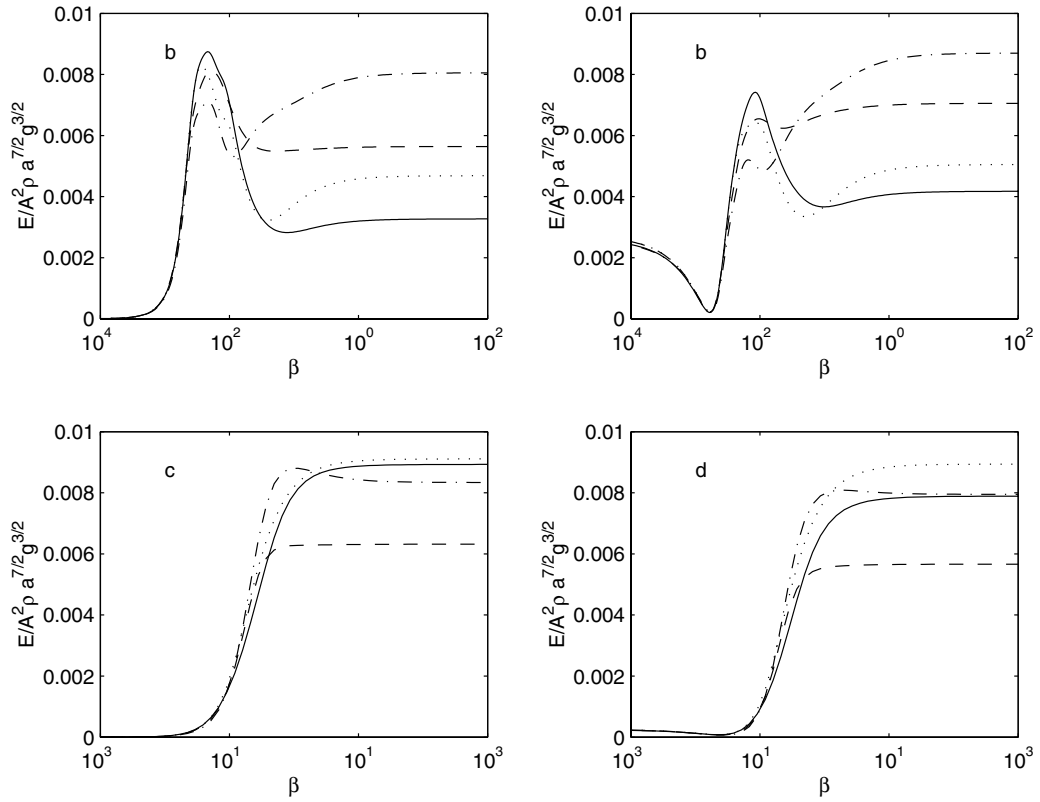


Figure 8. The total scattering as a function of β for ice floe geometries 1 (solid lines), 2 (dashed lines), 3 (dashed-dotted lines), and 4 (dotted lines). The wave number is (a and b) $\alpha = \pi$ and (c and d) $\alpha = \pi/2$ and the mass is (a and c) $\gamma = 0$ and (b and d) $\gamma = 0.005$.

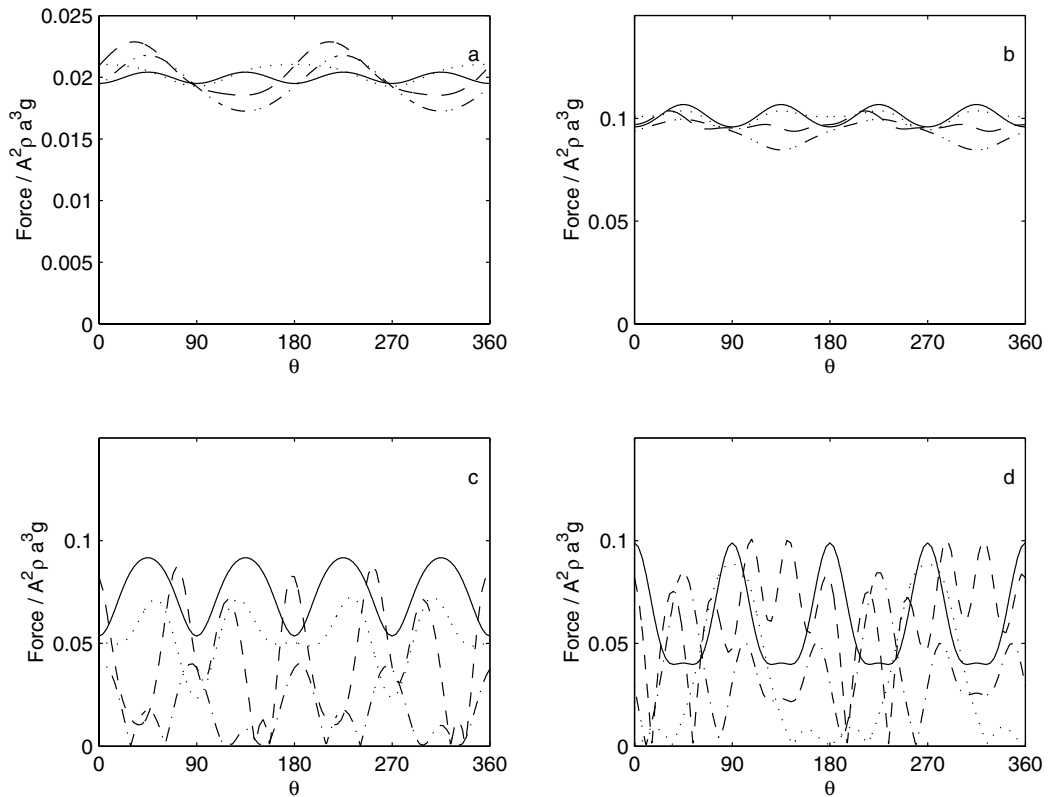


Figure 9. The total force as a function of incoming wave angle for ice floe geometries 1 (solid lines), 2 (dashed lines), 3 (dashed-dotted lines), and 4 (dotted lines). The values of the stiffness are (a) $\beta = 0.0004$, (b) $\beta = 0.002$, (c) $\beta = 0.01$, and (d) $\beta = 0.05$, with $\gamma = 0.005$ and $\alpha = \pi$.

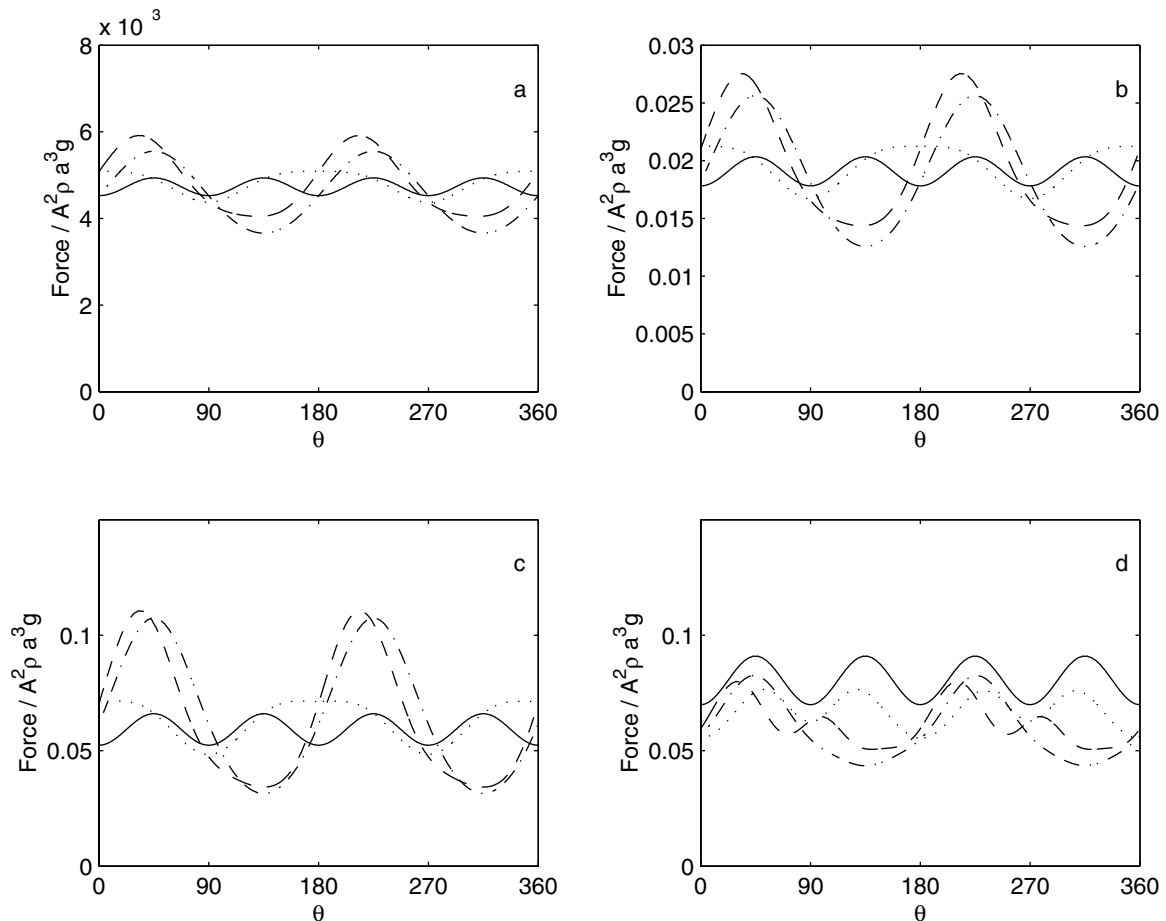


Figure 10. The total force as a function of incoming wave angle for ice floe geometries 1 (solid lines), 2 (dashed lines), 3 (dashed-dotted lines), and 4 (dotted lines). The values of the stiffness are (a) $\beta = 0.004$, (b) $\beta = 0.02$, (c) $\beta = 0.1$, and (d) $\beta = 0.5$, with $\gamma = 0.005$ and $\alpha = \pi/2$.

values λ_j) and solving the integral equations (12) and (13). We use the finite element method to determine the modes of vibration [Zienkiewicz and Taylor, 1989], and the integral equations (12) and (13) are solved by a constant panel method [Sarpkaya and Isaacson, 1981]. The same set of nodes is used for the finite element method and to define the panels for the integral equation.

5. Displacements

[23] We have developed a method to solve for the motion of an ice floe of arbitrary shape and properties due to waves of arbitrary frequency. While we will present the solutions in the nondimensional variables, we can still vary α , β , γ , and floe geometry. We are therefore able to only present a subset of possible solutions. We consider only the four ice floe geometries which are shown in Figure 2 (along with their numbering) which represent a range of floe geometries. We concentrate on the effect of the stiffness β rather than the mass γ . This is because the ice floes we consider are thin so that the mass term γ must necessarily be small (i.e., $1 - \alpha\gamma \approx 1$).

[24] Figure 3 is the displacement of an ice floe of geometry 1 to waves traveling in the x direction (this corresponds to $\theta = 0$ in (8)) with wave number $\alpha = \pi$ (this corresponds to a nondimensional wavelength of 2). The values of the stiffness are $\beta = 0.002$, 0.01, and 0.05, and the mass is $\gamma = 0.005$. The motion of the ice floe is a dynamic process in time, and the displacement at $t = 0$ and $t = T/4$ is plotted (these correspond to the real and imaginary parts of w , respectively). The solution was calculated with 40 free plate modes and 900 panels. These values were chosen by increasing the

number of modes and panels until the solution converges. Figures 4, 5, and 6 are the same as Figure 3 except the floe geometries are 2, 3, and 4, respectively. The ragged edges in Figures 4–6 arise because the geometries are approximated by square panels.

[25] Figures 3–6 show just how complicated the motion of an ice floe can be and how much this motion depends on details of the geometry of the ice floe. For example, the motion of the triangular floe (Figure 6) is far more complicated than the motion of the square floe (Figure 3). Obviously, this high dependence on individual geometry would not hold for floes which were much smaller or larger than the wavelength. Furthermore, since most ice floes have intermediate values of stiffness, the rigid body model is not appropriate.

6. Scattered Energy

[26] The wave energy scattering from the aggregate of ice floes that make up the MIZ is controlled by the scattering from individual floes. One of the problems in modeling wave propagation in the MIZ has been making an accurate determination of the scattering by an individual floe. The scattered energy can be expressed in terms of the Kochin function given by

$$H(\tau) = \iint_{\Delta} (\alpha\phi + i\sqrt{\alpha}w) e^{i\alpha(x\cos\tau + y\sin\tau)} dS \quad (16)$$

[Wehausen and Laitone, 1960] where ϕ and w are the complex potential and displacement, as before. The nondimensional radiated

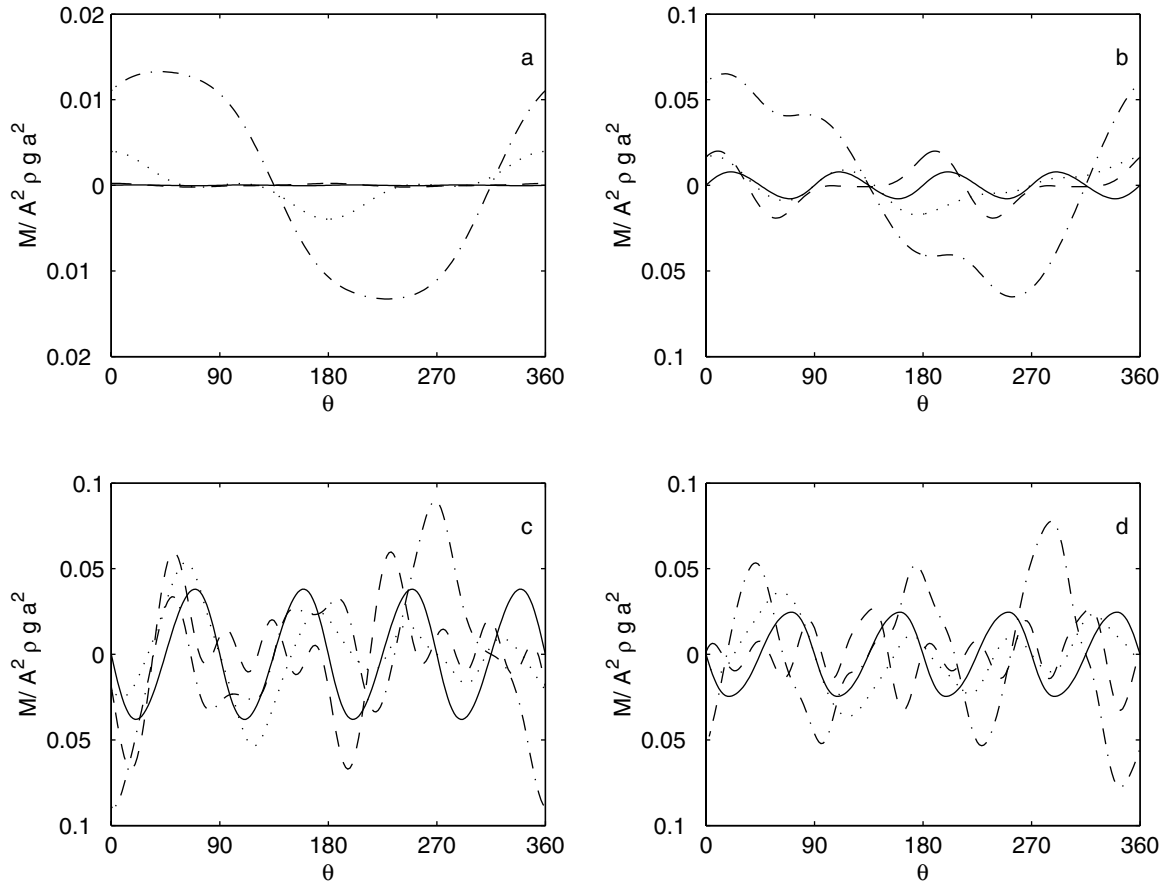


Figure 11. The yaw moment as a function of incoming wave angle for ice floe geometries 1 (solid lines), 2 (dashed lines), 3 (dashed-dotted lines), and 4 (dotted lines). The values of the stiffness are (a) $\beta = 0.0004$, (b) $\beta = 0.002$, (c) $\beta = 0.01$, and (d) $\beta = 0.05$, with $\gamma = 0.005$ and $\alpha = \pi$.

energy for a wave of unit amplitude, per unit angle, per unit time, in the τ direction is

$$\frac{E(\tau)}{A^2 \rho a^{7/2} g^{3/2}} = \frac{\alpha^3}{A^2 8\pi} |H(\pi + \tau)|^2$$

[Wehausen and Laitone, 1960]. This is the wave energy which is generated by the motion of the floe.

[27] The scattered energy $E(\tau)$ is also a function of the incoming wave angle θ . To avoid plotting $E(\tau)$ for different values of θ , we average the scattering over the difference in angle $\tau - \theta$. We expect the wave scattering in the MIZ to be determined by such an averaging because, in general, ice floes do not appear to be aligned. Figure 7 shows the average scattered energy for the four ice floe geometries (the solid line is geometry 1, the dashed line is geometry 2, the dashed-dotted line is geometry 3, and the dotted line is geometry 4). The values of the stiffness are $\beta = 0.0004$ (Figure 7a), $\beta = 0.002$ (Figure 7b), $\beta = 0.01$ (Figure 7c), and $\beta = 0.05$ (Figure 7d). The mass is $\gamma = 0.005$.

[28] From Figure 7 we can see that the scattering is predominantly in the direction of the incoming wave. There is only significant scattering in the backward direction for higher values of β . While there is a significant increase in the scattering from $\beta = 0.0004$ to $\beta = 0.002$, there is little further increase, and for some geometries, there is a decrease, as β is increased further. For small values of stiffness the scattering is independent of floe geometry but for higher values of stiffness, there is significant variation in the scattering between the different geometries.

[29] To understand Figure 7 we plot the total scattered energy (the integral over all angles) as a function of β for the four floe geometries. The wave number was $\alpha = \pi$ (Figures 8a and 8b) and $\alpha = \pi/2$ (Figures 8c and 8d) with $\gamma = 0$ (Figures 8a and 8c) and $\gamma = 0.005$ (Figures 8b and 8d). Figure 8 shows that there is strong dependence of the scattered energy on the parameter β . There is also a clear value of β , below which floe geometry is unimportant and above which floe geometry has a significant effect. Furthermore, for geometries and wavelengths which are of a similar size (Figures 8a and 8b), there is a stiffness of maximum scattering. In the cases of nonzero mass (Figures 8b and 8d) the low β limit corresponds to the mass loading model of Keller and Weitz [1953] which assumes zero floe stiffness.

7. Time-Averaged Force

[30] The time-averaged wave force on the floe is second order, but it can be determined by the first-order solution we have calculated. The average force components, for a wave of unit amplitude, in the x and y directions are given by

$$\frac{X_{av}}{A^2 \rho a^3 g} = \frac{\alpha^2}{8\pi A^2} \int_0^{2\pi} |H(\tau)|^2 \cos \tau d\tau + \cos \theta \frac{\sqrt{\alpha}}{2A^2} \text{Im} [H(\pi + \theta)], \quad (17)$$

$$\frac{Y_{av}}{A^2 \rho a^3 g} = \frac{\alpha^2}{8\pi A^2} \int_0^{2\pi} |H(\tau)|^2 \sin \tau d\tau + \sin \theta \frac{\sqrt{\alpha}}{2A^2} \text{Im} [H(\pi + \theta)], \quad (18)$$

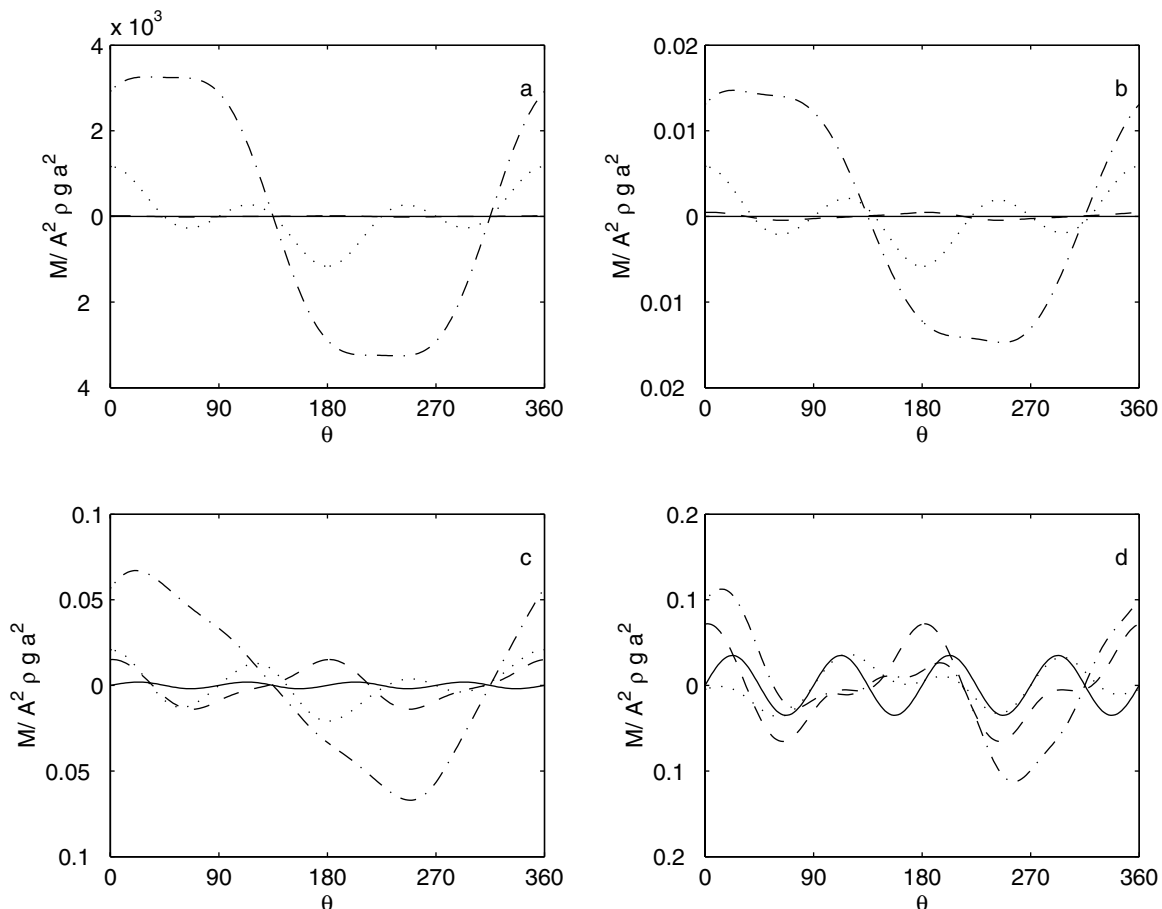


Figure 12. The yaw moment as a function of incoming wave angle for ice floe geometries 1 (solid lines), 2 (dashed lines), 3 (dashed-dotted lines), and 4 (dotted lines). The values of stiffness are (a) $\beta = 0.004$, (b) $\beta = 0.02$, (c) $\beta = 0.1$, and (d) $\beta = 0.5$, with $\gamma = 0.005$ and $\alpha = \pi/2$.

[Newman, 1967; Mauro, 1960]. There is a large variation in these components of force as a function of incoming wave direction, and we therefore consider the total force F given by

$$F = \sqrt{(X_{av})^2 + (Y_{av})^2}.$$

[31] Figure 9 shows the total force as a function of incident wave angle for the four values of stiffness $\beta = 0.0004$ (Figure 9a), 0.002 (Figure 9b), 0.01 (Figure 9c), and 0.05 (Figure 9d). The wave number is $\alpha = \pi$, and the mass is $\gamma = 0.005$. Like the scattering, below some value of β the force is independent of geometry, and above it, geometry is significant. Figure 10 shows the total force as a function of incident wave angle for the four values of stiffness $\beta = 0.004$ (Figure 10a), 0.02 (Figure 10b), 0.1 (Figure 10c), and 0.5 (Figure 10d). The wave number is $\alpha = \pi/2$ and the mass is $\gamma = 0.005$. Again, the variation of force with floe geometry is significant only for higher stiffness. However, the variation in force with wave angle is less for the smaller wave number (i.e., less in Figure 10 than in Figure 9).

[32] The final component of force which we consider is the average yaw moment on the body, which is given by

$$\frac{M_{av}}{\rho a^2 g} = -\frac{\alpha}{8\pi} \text{Im} \left[\int_0^{2\pi} H^*(\tau) H'(\tau) d\tau \right] - \frac{1}{2\sqrt{\alpha}} \text{Re}[H'(\pi + \theta)] \quad (19)$$

[Newman, 1967]. This moment is generally neglected in calculations of ice floe motions. However, the twisting of ice floes may be

a significant cause of floe collisions and may influence the total scattering by acting to align the floes. Figures 11 and 12 show the yaw moment for the four ice floe geometries for mass $\gamma = 0.005$ and wave number $\alpha = \pi$ (Figure 11) and $\alpha = \pi/2$ (Figure 12). The stiffness is $\beta = 0.0004$ (Figure 11a), $\beta = 0.002$ (Figure 11b), $\beta = 0.01$ (Figure 11c), and $\beta = 0.05$ (Figure 11d) and $\beta = 0.004$ (Figure 12a), $\beta = 0.02$ (Figure 12b), $\beta = 0.1$ (Figure 12c), and $\beta = 0.5$ (Figure 12d). The variation of yaw is markedly different for different geometries regardless of the wave number and stiffness. This is to be expected since the yaw moment is strongly dependent on the geometry of the floe. Figures 11 and 12 are hard to interpret, but it is apparent that for certain geometries the yaw is a significant force.

8. Geophysical Implications

[33] It is well known that significant wave scattering occurs in the marginal ice zone and that scattering plays an important role in controlling the breakup of pack ice. This wave scattering is controlled by the scattering from individual ice floes. We are now in a position to better understand wave scattering in the MIZ because we have a realistic model for individual ice floe scattering. This ice floe model is required for any MIZ scattering model such as the ones developed by *Masson and LeBlond* [1989] and *Meylan et al.* [1997]. The ice floe model also allows the wave-induced forces on ice floes to be calculated. This allows the drift and interfloe stress to be determined.

[34] From Figures 3–6 it is apparent that measurements of strain, displacement, or acceleration on an ice floe will be highly dependent on ice floe geometry and should be interpreted with extreme caution. Furthermore, if measurements are to be made, displacement or acceleration measurements will work better than strain because the variation in displacement is less than the variation in the second derivative of displacement.

[35] Figures 7–10 reveal that, for a given floe size, it is the ice floe stiffness, which depends predominantly on the floe thickness and to a lesser extent on the Young's modulus, which is the principle determinant of scattered energy and force. This means that these parameters, as well as average floe size, must be determined to accurately characterize the MIZ

[36] Furthermore, Figures 7–10 show that there is a critical stiffness, below which the scattering and force do not depend on floe geometry and above which the scattering and force do depend on floe geometry. The wave scattering or floe drift can therefore be calculated by considering a simple floe geometry (such as a circle) only for stiffness below the critical stiffness. It is interesting to consider some "typical" ice floes and to examine whether they lie above or below this critical stiffness. We take the following as the floe parameters: the density $\rho_i = 922.5 \text{ kg m}^{-3}$, the Young's modulus $E = 6 \text{ GPa}$, Poisson's ratio $\nu = 0.3$, and floe thickness $h = 1 \text{ m}$. If we consider a $40,000\text{-m}^2$ floe, then $\beta = 5.4752 \times 10^{-4}$, which puts it below the critical value for the wavelengths in Figure 8 (which are $\lambda = 100 \text{ m}$ (Figure 8a and 8b) and 200 m (Figure 8c and 8d)). However, for a $10,000\text{-m}^2$ floe, $\beta = 8.7604 \times 10^{-2}$, which is above the critical value of β for $\lambda = 100 \text{ m}$ and below for $\lambda = 200 \text{ m}$. Therefore typical floes lies in both regions, and care must be taken if only a simple floe geometry is to be considered.

9. Summary

[37] The wave-induced motion of a flexible ice floe of arbitrary geometry has been calculated. This solution was based on substituting the free modes of vibration of the ice floe into the integral equation which describes the water motion. Solutions were presented for four ice floe geometries and for two wave numbers. The complex nature of the motion of the ice floes was apparent as was the significance of flexure.

[38] The scattered energy was calculated, and it was shown that the scattering was most strongly dependent on ice floe stiffness. Further, it was shown that there exists a critical value of stiffness, below which the scattered energy is not a significant function of ice floe geometry and above which the average scattering is a significant function of ice floe geometry.

[39] Finally, the time-averaged forces acting on the ice floe were calculated. The total force showed a strong dependence on ice floe stiffness and also had a critical stiffness value above which floe geometry becomes significant. The results for the yaw moment were more difficult to interpret but showed that for certain ice floe geometries this force is significant.

References

- Abramowitz, M., and I. Stegun, *Handbook of Mathematical Functions*, Dover, Mineola, New York, 1964.
- Fox, C., and V. A. Squire, On the oblique reflexion and transmission of ocean waves a shore fast sea ice, *Philos. Trans. R. Soc. Lond., Ser. A.*, 347, 185–218, 1994.
- Hildebrand, F. B., *Methods of Applied Mathematics*, 2nd ed., Prentice-Hall, Englewood Cliffs, N. J., 1965.
- John, F., On the motion of floating bodies, I, *Commun. Pure Appl. Math.*, 2, 13–57, 1949.
- John, F., On the motion of floating bodies, II, *Commun. Pure Appl. Math.*, 3, 45–101, 1950.
- Keller, J. B., and M. Weitz, Reflection and transmission coefficients for waves entering or leaving an icefield, *Commun. Pure Appl. Math.*, 6, 415–417, 1953.
- Masson, D., Wave-induced drift force in the marginal ice zone, *J. Phys. Oceanogr.*, 21, 3–10, 1991.
- Masson, D., and P. LeBlond, Spectral evolution of wind-generated surface gravity waves in a dispersed ice field, *J. Fluid Mech.*, 202, 111–136, 1989.
- Mauro, H., The drift of a body floating on waves, *J. Ship Res.*, 4, 1–10, 1960.
- Meylan, M. H., and V. A. Squire, The response of ice floes to ocean waves, *J. Geophys. Res.*, 99, 891–900, 1994.
- Meylan, M. H., and V. A. Squire, Response of a circular ice floe to ocean waves, *J. Geophys. Res.*, 101, 8869–8884, 1996.
- Meylan, M. H., V. A. Squire, and C. Fox, Towards realism in modeling ocean wave behavior in marginal ice zones, *J. Geophys. Res.*, 102, 22,981–22,991, 1997.
- Newman, J. N., The drift force and moment on ships in waves, *J. Ship Res.*, 11, 51–60, 1967.
- Sarpkaya, T., and M. Isaacson, *Mechanics of Wave Forces on Offshore Structures*, Van Nostrand Reinhold, New York, 1981.
- Squire, V., and S. C. Moore, Direct measurement of the attenuation of ocean waves by pack ice, *Nature*, 283, 365–368, 1980.
- Squire, V. A., Dynamics of ice floes in sea waves, *J. Soc. Underwater Technol.*, 9, 20–26, 1983.
- Squire, V. A., and S. Martin, A field study of the physical properties, response to swell, and subsequent fracture of a single ice floe in the winter bearing sea, *Sci. Rep. 18*, Dep. of Atmos. Sci. and Oceanogr., Univ. of Wash., Seattle, 1980.
- Squire, V. A., J. P. Duggan, P. Wadhams, P. J. Rottier, and A. J. Liu, Of ocean waves and sea ice, *Annu. Rev. Fluid Mech.*, 27, 115–168, 1995.
- Wadhams, P., The seasonal ice zone, in *The Geophysics of Sea Ice*, edited by N. Untersteiner, pp. 825–991, Plenum, New York, 1986.
- Wadhams, P., V. A. Squire, J. A. Ewing, and R. W. Pascal, The effect of marginal ice zone on the directional wave spectrum of the ocean, *J. Phys. Oceanogr.*, 16, 358–376, 1986.
- Wadhams, P., V. A. Squire, D. J. Goodman, A. M. Cowan, and S. C. Moore, The attenuation rates of ocean waves in the marginal ice zone, *J. Geophys. Res.*, 93, 6799–6818, 1988.
- Wehausen, J. V., and E. V. Laitone, Surface waves, in *Fluid Dynamics, Handb. Phys.*, vol. 9, edited by S. Flugge, and C. Truesdell, pp. 446–778, Springer-Verlag, New York, 1960.
- Zienkiewicz, O. C., and R. L. Taylor, *The Finite Element Method*, vol. 1, 4th ed., McGraw-Hill, New York, 1989.

M. H. Meylan, Institute of Information and Mathematical Sciences, Massey University, Albany Campus, Private Bag 102 – 904 , Northshore Mail Center, Auckland, New Zealand. (m.h.meylan@massey.ac.nz)